JOURNAL OF VIROLOGY, Nov. 2007, p. 12169–12178 Vol. 81, No. 22
0022-538X/07/$08.00+0 doi:10.1128/JVI.00835-07

Lipid Raft Disruption by Cholesterol Depletion Enhances Influenza A Virus Budding from MDCK Cells[▽]

Subrata Barman and Debi P. Nayak*

Department of Microbiology, Immunology and Molecular Genetics, Jonsson Comprehensive Cancer Center, Molecular Biology Institute, David Geffen School of Medicine, University of California Los Angeles, Los Angeles, California 90095-1747

Received 18 April 2007/Accepted 6 September 2007

Lipid rafts play critical roles in many aspects of the influenza A virus life cycle. Cholesterol is a critical structural component of lipid rafts, and depletion of cholesterol leads to disorganization of lipid raft microdomains. In this study, we have investigated the effect of cholesterol depletion by methyl-β-cyclodextrin (MβCD) treatment on influenza virus budding. When virus-infected Madin-Darby canine kidney cells were treated with MβCD at the late phase of infection for a short duration, budding of virus particles, as determined by protein analysis and electron microscopy, increased with increasing concentrations and lengths of treatment. However, infectious virus yield varied, depending on the concentration and duration of MβCD treatment. Low concentrations of MβCD increased infectious virus yield throughout the treatment period, but higher concentrations caused an initial increase of infectious virus titer followed by a decrease with a longer duration. Relative infectivity of the released virus particles, on the other hand, decreased with increasing concentrations and durations of MβCD treatment. Loss of infectivity of virus particles is due to multiple effects of MβCD-mediated cholesterol depletion causing disruption of lipid rafts, changes in structural integrity of the viral membrane, leakage of viral proteins, a nick or hole on the viral envelope, and disruption of the virus structure. Exogenous cholesterol increased lipid raft integrity, inhibited particle release, and partially restored the infectivity of the released virus particles. These data show that disruption of lipid rafts by cholesterol depletion caused an enhancement of virus particle release from infected cells and a decrease in the infectivity of virus particles.

Lipid rafts are lipid microdomains enriched in sphingolipids and cholesterol. They contain lipids in liquid order (l_o) phase and are relatively resistant to nonionic detergent at a low temperature (6, 7, 44). Lipid rafts have been shown to play critical roles in many aspects of the virus life cycle, including viral entry and fusion, viral protein transport and targeting, and viral assembly and budding (26–28, 33, 41, 42).

Influenza A viruses are enveloped, segmented, negative-stranded RNA viruses and bud from the plasma membrane (more specifically, the apical plasma membrane of polarized epithelial cells). Virus particles consist of three major subviral components, namely, the viral envelope, the matrix protein (M1), and the core (viral ribonucleocapsid [vRNP]). The viral envelope surrounding the vRNP consists of a lipid bilayer containing transmembrane proteins (HA, NA, and M2) on the outer side and M1 on the inner side (28). Among the three influenza viral envelope proteins, HA and NA, but not M2, use lipid rafts as a platform for apical transport and remain associated with lipid raft microdomains present on cellular membranes (26, 27, 48). However, Schroeder et al. (43) recently reported that M2 is a cholesterol-binding protein and proposed that cholesterol association of M2 may play a critical role in virus budding. Furthermore, in the envelope of released virions, both HA and NA remain raft associated, whereas M2 does not associate with lipid rafts. These results indicate that the influenza viral envelope exhibits a mosaic mixture of both raft-associated and non-raft-associated lipid microdomains even though the majority of lipids present in the viral envelope are in the l_o phase and the influenza virus envelope is enriched in cholesterol-dependent detergent-insoluble lipids (39, 48). Furthermore, protein-protein interactions may facilitate bringing non-raft-associated proteins to lipid raft microdomains. For example, interactions of influenza virus M1 with HA and NA bring M1, a non-raft-associated protein, into lipid rafts (1). Recently, lipid rafts have been also proposed to be involved in transporting NP/vRNP to the apical side of polarized epithelial cells (9). By analyzing detergent-resistant lipid complexes in cellular membranes and viral envelopes, it has been shown that the influenza virus envelope is enriched in cholesterol-dependent detergent-insoluble lipids and that the lipids in the viral envelope are in a highly ordered state (39). Using recombinant influenza A virus containing mutant HA that does not associate with lipid rafts, Takeda et al. (47) observed reduced budding in cells infected with mutant virus compared to that seen with wild-type virus. These observations suggest that influenza viruses use lipid rafts as their budding platform. However, little is known about the role of lipid rafts in the budding process, specifically in bud release.

Cholesterol is a known critical structural component of lipid rafts. Depletion of cholesterol leads to disorganization of lipid raft microdomains and dissociation of proteins bound to the lipid rafts (15, 16, 40, 48). In this study, we have investigated the effect of cholesterol depletion, which leads to disruption of

* Corresponding author. Mailing address: Department of Microbiology, Immunology and Molecular Genetics, Jonsson Comprehensive Cancer Center, Molecular Biology Institute, David Geffen School of Medicine, University of California Los Angeles, Los Angeles, CA 90095-1747. Phone: (310) 825-8558. Fax: (310) 206-3865. E-mail: dnayak@ucla.edu.

▽ Published ahead of print on 12 September 2007.

lipid raft microdomains, on influenza virus budding. Since depletion of cholesterol by inhibition of cholesterol biosynthesis by use of drugs like lovastatin or squalestatin requires a longer time of incubation and therefore could affect other steps in virus life cycle, including viral protein transport (9, 20, 36), those drugs could not be used to examine the effect of cholesterol depletion on budding and virus release. On the other hand, cholesterol-binding agents such as digitonin, saponin, filipin, nystatin, or methyl-β-cyclodextrin (MβCD) can remove cholesterol and cause disruption of lipid rafts within a short period of time. However, unlike other cholesterol-binding agents that become incorporated into membranes, MβCD is a strictly surface-acting agent and can selectively and rapidly remove cholesterol from the plasma membrane in preference to other membrane lipids and has been widely used in studying the effects of cholesterol depletion and lipid raft disassembly (2, 13, 17, 18, 21–23, 29, 32, 35). We therefore chose MβCD as a cholesterol-depleting agent and treated virus-infected Madin-Darby canine kidney (MDCK) cells with MβCD for short durations at the late phase of infection to avoid the effect of lipid raft disruption on protein transport (9, 20, 36) and virus assembly (24, 39, 47, 48). The results show that depletion of cholesterol from virus-infected cells by MβCD treatment facilitated bud completion and increased virus particle release. However, depletion of cholesterol from virus particles by MβCD treatment caused disruption of lipid rafts on viral membranes, loss of infectivity of virus particles, nicks or holes on the viral envelope and disruption of particle structure, and release of viral proteins. Finally, we show that incubation of cells with exogenous cholesterol can restore lipid raft integrity and inhibit virus particle release.

MATERIALS AND METHODS

Cell lines, viruses, and plaque assay. MDCK cells were maintained in minimum essential medium (Invitrogen, Rockville, MD), and influenza virus (A/WSN/33, H1N1) stock was prepared in MDCK cells as described previously (4). Assays for PFU were described earlier (4).

[^{3}H]-cholesterol labeling of cells and extraction with cyclodextrins (CDs). MDCK cells were grown on 24-well plates for 20 h, labeled with 5 μCi/ml [1α,2α-^{3}H]-cholesterol (Sigma, St. Louis, MO) in virus growth medium (VGM; minimum essential medium containing 0.2% bovine serum albumin, 4% basal medium Eagle vitamins, 10 mM HEPES [pH 7.2], 0.155% $NaHCO_3$, 0.0015% DEAE-dextran, 100-U/ml penicillin G, 100-μg/ml streptomycin) for 18 h, and treated with different concentrations of MβCD or HβCD [(2-hydroxypropyl)-β-CD] or HγCD [(2-hydroxypropyl)-γ-CD] (Sigma) in VGM. Levels of ^{3}H-cholesterol released to the media and ^{3}H-cholesterol remaining in cells (unreleased) were assayed by liquid scintillation counting (8). Percentages of ^{3}H-cholesterol released were calculated by the following equation: 100 × (released fraction)/(released fraction + unreleased fraction).

Release of infectious virus particles from virus-infected cells after MβCD treatment. MDCK cell monolayers (35 mm dish, 2×10^6 cells) were infected with influenza virus at a multiplicity of infection (MOI) of 3 and treated with 10 mU/ml of bacterial neuraminidase (NA) (Calbiochem, San Diego, CA) in VGM from 10 to 12 h p.i. to remove virus particles attached to the cell surface (4); they were washed five times with PBS$^+$ (PBS supplemented with $0 \cdot 5$ mM $MgCl_2$ and 1 mM $CaCl_2$) and once with VGM. The cells were then mock treated or treated with different concentrations of MβCD in 1.5 ml of VGM for various lengths of time, and infectious virus particles released into the medium were quantified by PFU assay.

Analysis of ^{35}S-labeled virus particles released from infected cells. MDCK cells infected with virus at an MOI of 3 were labeled with ^{35}S-protein labeling mix (Perkin-Elmer Life Sciences, Boston, MA) for 8 h (4 to 12 h p.i.) and treated with bacterial NA from 10 to 12 h p.i. At 12 h p.i., the infected cells were washed six times and either mock treated or treated with different concentrations of MβCD, HβCD, or HγCD in 1.5 ml of VGM. Media were harvested at indicated times, cell debris was removed by microcentrifuge (16,000 × g, 10 min at 4°C), and virus particles were concentrated and purified by ultracentrifugation (Beckman SW 50.1Ti rotor, 35,000 rpm, 2.5 h) through a 25% sucrose cushion (4). Viral proteins in the pellet were analyzed by sodium dodecyl sulfate-polyacrylamide gel electrophoresis (SDS-PAGE) and autoradiographed. Radioactive protein bands were detected by storage phosphorimaging with a PhosphorImager (Typhoon 9410) and quantified using ImageQuant software (Amersham Biosciences, Piscataway, NJ). To examine the release of virus particles from MβCD-treated cells but without MβCD in the medium, the infected cells were labeled with ^{35}S-protein labeling mix (4 h p.i. to 11 h 15 min p.i.) and treated with bacterial NA (10 h p.i. to 11 h 15 min p.i.); at 11 h 15 min p.i., they were treated with different concentrations of MβCD along with bacterial NA in 1.5 ml of VGM for 45 min. At 12 h p.i., the cells were washed as before and incubated in 1.5 ml of VGM without MβCD. After 45 min of incubation, cell culture supernatants were harvested; released infectious viruses were quantified by PFU assay; and total particle release was assayed by protein analysis as mentioned above.

MβCD treatment of virus particles. MDCK cells infected with virus at an MOI of 3 were metabolically labeled with ^{35}S-protein labeling mix for 8 h (4 to 12 h p.i.), and released virions were purified (4) and resuspended in VGM. ^{35}S-labeled virus particles were either mock treated or treated with different concentrations of MβCD or HβCD for various lengths of time at 37°C; aliquots were diluted in ice-cold virus dilution buffer (VDB, phosphate-buffered saline [PBS] supplemented with 0.5 mM $MgCl_2$, 1.0 mM $CaCl_2$, 50 μg of DEAE-dextran/ml, and 0.2% bovine serum albumin) for PFU assay. Other aliquots were diluted with ice-cold TNE buffer (10 mM Tris-HCl [pH 7.4], 100 mM NaCl, and 1.0 mM EDTA) and were pelleted again by a second ultracentrifugation (Beckman SW 50.1Ti rotor, 4°C, 40,000 rpm, 2.5 h). The pellets and the supernatants were immunoprecipitated with the respective antibodies, analyzed by SDS-PAGE, and quantified.

Assay for TX-100 insolubility. At 12 h p.i. ^{35}S-labeled virus-infected MDCK cells were mock treated or treated with different concentration of MβCD or cholesterol-MβCD for 45 min. For some experiments, cells were treated first with 20 mM MβCD at 11 h 15 min p.i. for 45 min and then further mock treated or treated with cholesterol (0.62 mg/ml)-MβCD (10 mM). To evaluate the Triton X-100 (TX-100) insolubility of cell surface proteins, cells were biotinylated and then extracted with 1% TX-100 (Roche, Mannheim, Germany) in TNE buffer on ice for 10 min as described previously (4, 5). Both TX-100-soluble and -insoluble fractions were immunoprecipitated with specific antibodies. Biotinylated cell surface HA and NA were isolated by a second precipitation with streptavidin, analyzed by SDS-PAGE, autoradiographed, and quantified.

To determine the TX-100 insolubility of different proteins in the virus particles, 0.1% TX-100 (instead of 1.0% as used for treating infected cells) was used, since it was shown earlier that the TX-100 resistance of different proteins in virus particles was much lower than that of proteins present in cellular membranes (4, 5, 48). Virus particles released from MβCD-treated cells either with or without MβCD in medium were purified by ultracentrifugation through a sucrose cushion. Purified virions were extracted with 0.1% TX-100 (200 μl final volume in TNE buffer) on ice for 10 min, diluted to 5 ml ice-cold TNE buffer, and ultracentrifuged (Beckman SW 50.1Ti rotor, 4°C, 40,000 rpm, 2.5 h) (4). TX-100-soluble and -insoluble proteins were immunoprecipitated using the respective antibodies, analyzed by SDS-PAGE, and autoradiographed or quantified.

Treatment with exogenous cholesterol. In these experiments, water-soluble cholesterol (Sigma; 45 mg cholesterol complexed with 955 mg of MβCD [formula weight, 1320]) was used. To prepare different concentrations of cholesterol combined with a fixed concentration (10 mM) of MβCD, a cholesterol solution (0.62 mg/ml) containing 10 mM MβCD in VGM was mixed with various amounts of 10 mM MβCD alone in VGM. At 12 h p.i.; ^{35}S-labeled virus-infected cells were mock treated or treated with various concentrations of cholesterol containing MβCD in 1.5 ml of VGM for 45 min. Released virus particles were quantified by both PFU assay and protein analysis as described above. To replenish cholesterol in cholesterol-depleted cells, ^{35}S-labeled cells were treated (at 11 h 15 min p.i.) with 20 mM MβCD along with bacterial NA in 1.5 ml of VGM for 45 min. At 12 h p.i., the cells were further incubated with (or without) 0.62 mg/ml cholesterol containing 10 mM MβCD in 1.5 ml of VGM for 45 min. The released virus particles were quantified by both PFU assay and protein analysis.

Cellular cholesterol content measurement. Cellular cholesterol content was measured using an Amplex Red cholesterol assay kit (Invitrogen) according to manufacturer protocols and as described elsewhere (11). Briefly, mock- or MβCD- or cholesterol-MβCD-treated MDCK cells (35 mm dish, 2×10^6 cells) were harvested in 75 μl of PBS, lysed by three cycles of freezing and thawing, and extracted with 400 μl of chloroform-methanol (2:1). After 10 min of microcentrifugation, the bottom (chloroform) layer was collected and 200 μl aliquots were evaporated in a vacuum. The sample was dissolved in 25 μl of 2-propanol

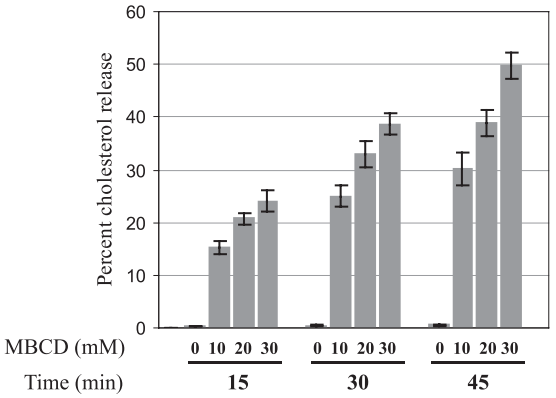

FIG. 1. Cholesterol release from MDCK cells resulting from MβCD treatment. Error bars, standard deviations (SD) ($n = 4$).

containing 10% TX-100, and a 0.8 μl sample was assayed with an Amplex Red cholesterol assay kit using a 96-well plate. All reactions were performed in duplicate.

Negative-stain EM. Electron microscopy (EM) was performed essentially as described elsewhere (19). Purified virions in PBS were mixed with latex beads (polystyrene; Sigma) that had an average diameter of 1.0 μm and were absorbed onto carbon-coated copper grids for 5 min. Grids were negatively stained with 2% phosphotungstic acid (pH 6.6) and examined with a JEOL JEM-100CX electron microscope (JEOL Ltd., Tokyo, Japan). For quantification, random fields were photographed at a magnification of ×19,000, and a portion of that field was further photographed at a magnification of ×72,000 to study virus morphology.

To examine the effect of MβCD or HβCD treatment on virus morphology, purified virions were treated with different concentrations of drugs and examined (magnification of ×36,000) as described above.

Thin-section electron microscopy. Cells (grown on polycarbonate filter) infected with virus at an MOI of 3 were treated with bacterial NA (10 to 12 h p.i.) and, at 12 h p.i., were mock treated or treated with 30 mM MβCD for 45 min. These cells were then cross-linked in 2% glutaraldehyde (EM grade) in PBS^+ and postfixed with 1% osmium tetraoxide in PBS^+. Filters were dehydrated, cut out from filter units, and embedded in Epon. Ultra-thin (60 nm) sections were stained with uranyl acetate and lead citrate and then examined with a JEOL JEM-100CX electron microscope (4).

RESULTS

Removal of cholesterol from MDCK cells by MβCD treatment. To determine the effect of MβCD on the removal of cholesterol, ^{3}H-cholesterol-labeled MDCK cells were treated with different concentrations of MβCD for various lengths of time, and the amounts of ^{3}H-cholesterol released in the media and remaining in cells (unreleased) were assayed as described in Materials and Methods. The results (Fig. 1) showed that increasing amounts of cholesterol were released into the medium with increasing concentrations and longer treatment of MβCD. Fifty percent of the cholesterol was released after 45 min of treatment with 30 mM MβCD (Fig. 1). Similar reductions of cellular cholesterol content were observed when total cholesterol was measured using a cholesterol assay kit (data not shown). Cell viability, integrity, and morphology and total cell numbers remained essentially unaffected when MDCK cells were treated with 30 mM MβCD for a maximum duration of 45 min. These results are consistent with previous observations of the effects of MβCD in MDCK cells (8, 9, 12, 25, 34, 38).

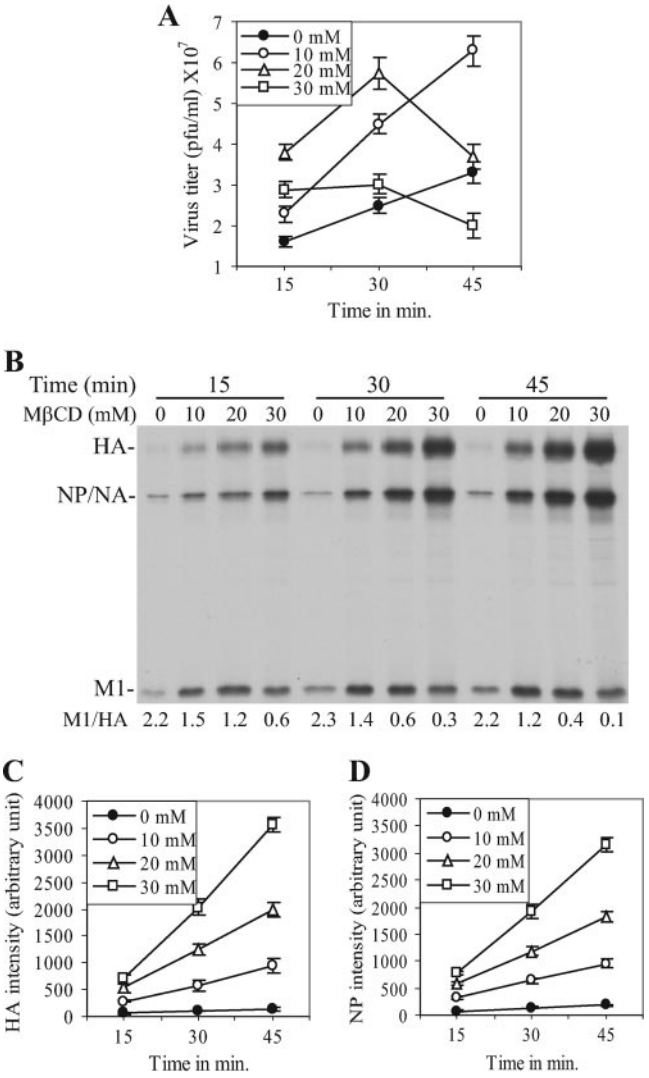

FIG. 2. Effect of MβCD treatment on virus budding. (A) PFU titers of viruses released from virus-infected (MOI of 3) MDCK cells after MβCD treatment (at 12 h p.i.). (B) ^{35}S-labeled virus particles released from MβCD-treated (at 12 h p.i.) cells were purified, and viral proteins were separated in SDS-PAGE. M1/HA ratios are shown at the bottom of the panel. (C and D) Intensities of the HA (C) and NP (D) protein bands shown in panel B are plotted in arbitrary units against durations (in minutes) of MβCD treatment. Error bars in panels A, C, and D, SD ($n = 5$).

Cholesterol depletion in virus-infected MDCK cells by MβCD treatment caused enhancement of virus budding. To investigate the effect of cholesterol depletion by MβCD treatment on influenza virus budding, virus-infected MDCK cells at the late phase of infection (12 h postinfection [p.i.]) were treated with different concentrations of MβCD for various lengths of time, and amounts of infectious virus released into the medium were quantified by PFU assay. The results (Fig. 2A) show that the PFU titer of the released virus particles varied depending on the concentration and duration of MβCD treatment. Treatment with 10 mM MβCD caused an increase in the yield of infectious virus titer throughout the duration (45 min) of treatment. However, higher concentrations of MβCD

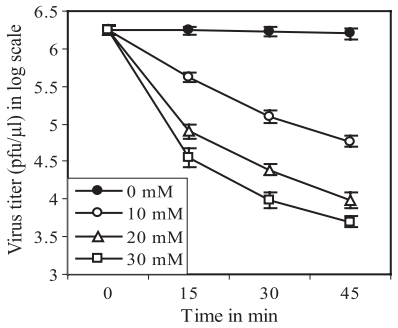

FIG. 3. Effect of MβCD treatment on infectivity of virus particles. Error bars, SD (n = 4).

caused an initial increase followed by a decrease in PFU titers with longer duration of treatment (Fig. 2A).

Since cholesterol depletion from virions was shown to reduce significantly the infectivity of influenza A viruses (46, 47) as well as of human immunodeficiency virus type 1 (HIV-1) and simian immunodeficiency virus (SIV) (14), it is possible that released virus particles became inactivated because of the continued presence of MβCD in the medium and that PFU titers may not have reflected total virus particle release. We therefore examined the amounts of particle released after MβCD treatment by protein analysis of ^{35}S-labeled released virus particles. The results (Fig. 2B) show that the particle release increased with increasing concentration and length of MβCD treatment as measured by HA and NP band intensity. Quantification of either HA (Fig. 2C) or NP (Fig. 2D) showed that particle release continued to increase with increasing concentrations and durations of MβCD treatment. It should be noted that NA, which migrates as a diffuse band of low intensity, comigrates with NP. It should be further noted that in the absence of exogenous proteases like trypsin, less than 10% of HA in released virus particles become cleaved. Therefore, we routinely quantified only the uncleaved HA (HA0) (this will be referred to as HA throughout the article). However, the amounts of M1 in the released virus particles varied and the ratio of M1/HA decreased in released virus particles with increasing concentrations and durations of MβCD treatment (Fig. 2B). Essentially, results were similar when ratios of M1/NP were determined (data not shown). The reason for the decreased M1/HA (or M1/NP) ratios in released virus particles is discussed later. Overall, the data presented in Fig. 2 show that based on the analysis of HA and NP levels, budding of virus particles increased with increasing concentrations and durations of MβCD treatment, although the titer of infectious viruses decreased with prolonged treatment at higher concentrations of MβCD.

TABLE 1. Proteins released from virus particles after MβCD treatment[a]

MβCD concn (mM)	Mean (SD) % of proteins released			
	HA	NA	NP	M1
0	5.1 (0.4)	5.7 (0.4)	3.7 (0.3)	4.5 (0.3)
10	11.8 (0.6)	12.1 (0.8)	29.3 (1.7)	53.7 (3.8)
20	13.7 (0.4)	14.2 (0.6)	33.5 (1.6)	55.1 (3.2)
30	20.7 (1.2)	19.5 (1.0)	36.7 (2.3)	56.3 (3.7)

[a] ^{35}S-labeled virus particles were either mock treated (0 mM MβCD) or treated with the indicated concentrations of MβCD at 37°C for 30 min, and viral proteins released and remaining in the virions were separated by ultracentrifugation. Data are presented as mean (SD) (n = 3).

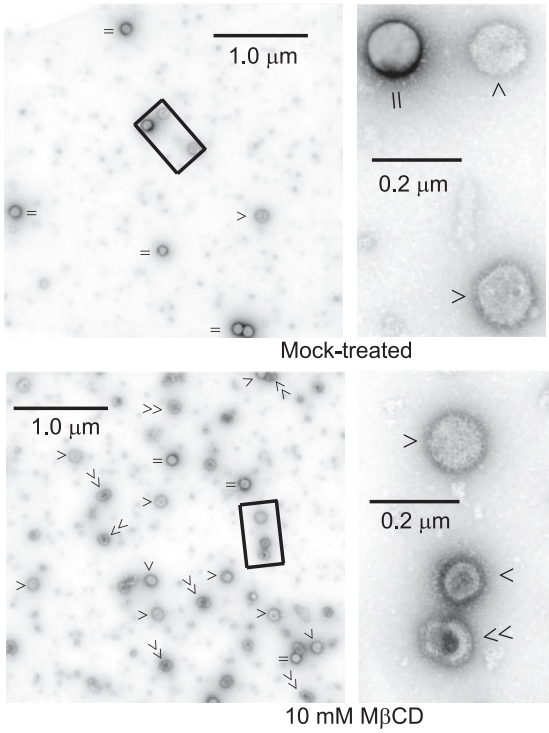

FIG. 4. Increased release of virus particles from MβCD-treated cells by negative stain EM. Virus particles released from mock- or MβCD-treated (for 45 min at 12 h p.i.) virus-infected (MOI of 3) MDCK cells were purified and examined by negative-stain EM. A portion of a representative micrograph is shown on the left (magnification, ×19,000). The rectangle on the left is magnified (×72,000) on the right. ‖ or =, beads; single arrowheads, normal virus particles; double arrowheads, disrupted virus particles.

Effect of MβCD on the infectivity of virus particles. Since infectious virus titers decreased for cells treated with higher concentrations and longer durations of MβCD, we examined the effect of the presence of MβCD on the infectivity of cell-free virus particles. The results (Fig. 3) show that MβCD treatment significantly reduced virus infectivity (more than 2 logs after 45 min treatment with 30 mM MβCD), indicating that the reduction of PFU titers at higher concentrations with longer treatment of MβCD (Fig. 2A) was at least partly because of the loss of infectivity of the released virus particles in the continued presence of MβCD in the medium. Furthermore, it has been reported that cholesterol depletion caused permeabilization of virions and release of viral proteins from HIV-1 and SIV particles (14). Therefore, we examined whether MβCD treatment caused release of viral proteins from influenza virus particles. The results (Table 1) show that unlike mock-treated (0 mM) virus sample results, increasing amounts of HA, NA, NP, and M1 were released from virus particles upon treatment with increasing concentrations of MβCD. M1 was released most (Table 1), which was the likely cause for lower M1/HA (or M1/NP) ratios in virus particles released from MβCD-treated cells (Fig. 2B). Furthermore, it

TABLE 2. Increased release of virus particles from MβCD-treated cells as determined by electron microscopy[a]

MβCD concn (mM)	No. of fields used	Mean (SD) no. of virus particles per field	Mean (SD) no. of beads per field	Mean (SD) no. of virus particles per bead	Relative increase of virus particle release
0	37	4.4 (0.9)	5.1 (1.0)	0.9 (0.2)	1
10	31	55.2 (9.3)	4.9 (1.1)	11.2 (2.7)	12.6

[a] Virus particles released from mock-treated or 10 mM MβCD-treated (at 12 h p.i. for 45 min) cells were examined by negative-stain EM, and identifiable virus particles as well as beads from electron micrographs (magnification, ×19,000) were counted. The results were obtained from three independent experiments with duplicate grids.

should be noted that the amount of virus particles released after MβCD treatment was probably higher than that observed by viral protein analysis of the released particles (Fig. 2B, C, and D) because even HA and NP were also partially released from virus particles after MβCD treatment (Table 1).

Therefore, we used another independent method, that is, negative-stain EM, to quantify particle release and examine the morphology of released particles. EM micrograph assays of virus particles collected after 10 mM MβCD treatment (45 min) showed an increased release of virus particles (Fig. 4). The EM micrographs also show that the majority of particles released from cells even after treatment with low concentrations (10 mM) of MβCD exhibited partially disrupted morphology (Fig. 4); such disruption was severe at higher concentrations (30 mM) of MβCD (data not shown). Quantification of the virus particles in those micrographs showed (Table 2) that after treatment of virus-infected cells with 10 mM MβCD for 45 min, virus particle release was significantly higher than that estimated by protein analysis (12.6-fold by EM versus 7.5-fold by protein analysis; Table 2 and 3).

Data presented in Fig. 2, 3, and 4 indicate that the lower infectivity of the virus particles released from MβCD-treated cells was at least partly caused by the continued presence of MβCD in the medium during drug treatment. Therefore, we examined the release of virus particles from MβCD-treated cells without MβCD in the medium. The results (Table 3) show that increased particle release from MβCD-treated cells continued even when MβCD was absent in the medium, albeit at a lower rate than that seen during MβCD treatment. The relative infectivity of the released particles, on the other hand, was higher when MβCD was absent in the medium (Table 3), although the relative infectivity of these virus particles still did not reach the same level (1.0) as that seen with the mock-treated cells. These results indicate that particles released from cholesterol-depleted cells also had reduced infectivity.

Cholesterol depletion by MβCD treatment caused disruption of lipid rafts. Depletion of cholesterol is expected to disrupt lipid raft microdomains, which can be distinguished from intact lipid rafts by a decrease in TX-100 insolubility of raft-associated proteins. Therefore, we examined the effect of cholesterol depletion on TX-100 insolubility of viral proteins in infected cells as well as in released virions. The results (Table 4) show that in cells treated with 10 mM, 20 mM, and 30 mM MβCD for 45 min, the levels of TX-100 insolubility of cell surface HA were reduced to 42%, 33%, and 27%, respectively, compared with the 61% insoluble HA seen in mock-treated cells. Similarly, the TX-100 insolubility of cell surface NA was also reduced (Table 4). These data indicate that cholesterol depletion by MβCD treatment caused disruption of lipid rafts. On the other hand, cholesterol depletion did not significantly affect the TX-100 insolubility of NP and M1 in infected cells. It is known that the TX-100 insolubility of NP is due to its interaction with actin cytoskeletons. Similarly, the TX-100 insolubility of M1 in infected cells is mostly due to its interaction with actin via vRNP (3) and a relatively small fraction of M1 becomes raft associated due to its interaction with HA and NA (1).

To determine whether MβCD treatment of infected cells also affected lipid rafts of released virus particles, the TX-100 insolubility of different viral proteins in virions collected after 45 min of treatment with different concentrations of MβCD was determined as described in Materials and Methods. The results (Table 4) show that HA, NA, and M1 were highly TX-100 soluble in the virions collected from virus-infected MβCD-treated cells. Because NP inside the virus particles remained as a vRNP complex (3), its TX-100 insolubility was

TABLE 3. Release of virus particles from MβCD-treated cells with or without MβCD in the medium

MβCD concn (mM)	Mean (SD) value in the absence of MβCD in the medium ($n = 4$)[a]				Mean (SD) value in the presence of MβCD in the medium ($n = 5$)[b]			
	Relative PFU titer	Relative particle release	Relative infectivity	M1/HA ratio	Relative PFU titer	Relative particle release	Relative infectivity	M1/HA ratio
0	100[c]	100	1.0	2.2 (0.13)	100[d]	100	1.0	2.2 (0.1)
10	330 (15)	611 (21)	0.54 (0.04)	1.5 (0.12)	195 (13)	750 (17)	0.26 (0.02)	1.2 (0.05)
20	332 (13)	955 (33)	0.35 (0.03)	1.0 (0.08)	134 (8)	1460 (64)	0.09 (0.01)	0.4 (0.02)
30	202 (12)	1130 (47)	0.18 (0.05)	0.8 (0.07)	66 (6)	2310 (87)	0.029 (0.002)	0.1 (0.01)

[a] At 11 h 15 min p.i., ^{35}S-labeled virus-infected cells were treated with different concentrations of MβCD for 45 min. At 12 h p.i., cells were washed six times and incubated in VGM without MβCD. After 45 min of incubation, released infectious viruses were quantified by PFU assay and total particle release was assayed by protein analysis. Relative values of PFU titer and relative particle release as a measure of HA protein band intensities were calculated as a percentage of the values obtained with mock-treated (0 mM) cells. Values of relative infectivity of virus particles were calculated as follows: [(relative PFU titer)/(relative particle release)].

[b] Data were taken from the results of the experiment represented in Fig. 2.

[c] $[6.54\ (0.5)] \times 10^7$ PFU/ml.

[d] $[6.84\ (0.4)] \times 10^7$ PFU/ml.

TABLE 4. TX-100 insolubility of viral proteins in MβCD-treated virus-infected cells and in released virions[a]

Protein and MβCD concn (mM)	Mean (SD) % of TX-100-insoluble proteins		
	Infected cells	Released virions collected:	
		With MβCD in medium	Without MβCD in medium
HA			
0	61 (3)		91 (4)
10	42 (3)	56 (3)	ND[b]
20	33 (2)	32 (2)	76 (3)
30	27 (2)	21 (2)	63 (3)
NA			
0	54 (3)		85 (5)
10	50 (4)	40 (3)	ND
20	37 (3)	32 (3)	68 (4)
30	28 (2)	16 (2)	49 (3)
NP			
0	35 (2)		94 (4)
10	30 (3)	81 (5)	ND
20	28 (2)	79 (3)	84 (4)
30	24 (2)	75 (4)	80 (3)
M1			
0	55 (3)		89 (3)
10	55 (3)	41 (3)	ND
20	53 (2)	25 (2)	82 (3)
30	53 (4)	17 (2)	76 (4)

[a] TX-100 insolubility of proteins (HA and NA surface proteins) in virus-infected MβCD-treated (for 45 min at 12 h p.i.) MDCK cells as well as in released virions with or without MβCD in the medium (as described in Table 3) was assayed as described in Materials and Methods. Values are presented as percentages of TX-100-insoluble proteins ($n = 4$).
[b] ND, not done.

not markedly affected by MβCD treatment. On the other hand, our data indicate that the TX-100 insolubility of M1 in virus particles depended on its association with HA and NA. In any case, the TX-100 insolubility of NP and M1 does not have much relevance to the interpretation of data presented here since those are not lipid raft-associated proteins.

Because MβCD was also present in the medium, it was not clear whether the increased TX-100 solubility of HA and NA in virions resulted from cholesterol depletion of the budding cellular membrane or cholesterol depletion of the virions after their release into the medium or both. Therefore, we analyzed the TX-100 insolubility of the proteins in virions that were collected from MβCD-treated cells without MβCD in the medium. The results (Table 4) show that the TX-100 insolubility of HA and NA was significantly higher in particles collected in the absence of MβCD in the medium compared to that of the virus particles collected with MβCD in the medium. The total cholesterol content of the cells as well as the TX-100 insolubility of surface HA and NA did not change significantly (see Table 7) after 45 min incubation of cholesterol-depleted cells in VGM, indicating that any endogenous synthesis of cholesterol within this short time (45 min) was not responsible for the increased TX-100 insolubility of HA and NA in virions released during a drug-free chase of cholesterol-depleted cells (i.e., virions collected without MβCD in the medium). Rather, these data support the idea that the increased TX-100 solubility of proteins in the virions collected with MβCD in the medium (Table 4) was partly caused by the effect of MβCD on released virus particles.

TABLE 5. Inhibition of virus release by endogenous cholesterol[a]

Cholesterol (mg/ml)	MβCD concn (mM)	Mean (SD) relative PFU titer	Mean (SD) relative particle release	Mean (SD) relative infectivity
0	0	100[b]	100	1
0	10	219 (8)	847 (21)	0.26 (0.02)
0.2	10	227 (8)	367 (7)	0.62 (0.03)
0.3	10	71 (0.5)	123 (3)	0.58 (0.05)
0.4	10	21 (0.2)	24 (1.2)	0.87 (0.07)
0.5	10	1.6 (0.13)	2.1 (0.17)	0.76 (0.06)
0.62	10	0.4 (0.03)	0.6 (0.1)	0.67 (0.07)

[a] At 12 h p.i., ^{35}S-labeled virus-infected cells were mock treated or treated with VGM containing different concentrations of cholesterol along with 10 mM MβCD for 45 min. Released infectious viruses were quantified by PFU assay, and total particle release was assayed by protein analysis. Values for relative PFU titer and relative particle release (HA protein band intensity) are presented ($n = 3$).
[b] [6.78 (0.27)] × 10^7 PFU/ml.

Effect of exogenous cholesterol on particle release and lipid raft integrity. To determine whether the effects of the drug (MβCD) were due solely to cholesterol depletion, we examined the effect of exogenous cholesterol on virus release during MβCD treatment of infected cells. Accordingly, ^{35}S-labeled virus-infected cells were treated at 12 h p.i. with different concentrations of cholesterol in the presence of 10 mM MβCD and virus release was examined by PFU assay (for infectious particles) as well as by protein analysis of released labeled virus particles. The results show (Table 5) that exogenous cholesterol inhibited the enhanced release of virus particles in an essentially dose-dependent manner and that 0.62 mg/ml of cholesterol containing 10 mM MβCD inhibited virus release by more than 2 logs compared to mock-treated cell results. Furthermore, cholesterol-MβCD caused a significant increase in the relative infectivity of released virus particles compared to that seen when cells were treated with MβCD only, indicating that exogenous cholesterol could partially restore the infectivity of released virus particles. We further investigated whether exogenous cholesterol can inhibit virus release from cholesterol-depleted cells. Accordingly, ^{35}S-labeled virus-infected cells were treated with 20 mM MβCD for 45 min. Cells were then washed and further treated with cholesterol (0.62 mg/ml)-MβCD (10 mM) or mock treated (no cholesterol, no MβCD) for 45 min. Virus release was examined by PFU assay as well as by protein analysis. The results (Table 6) show that the exogenous cholesterol also inhibited the release of virus particles from cholesterol-depleted cells. These results show that the increased release of virus particles after MβCD treatment (Fig. 2) was due to cholesterol depletion.

The above-described results show that lipid raft disruption by MβCD-mediated cholesterol depletion caused an increased release of virus particles. On the other hand, exogenous cholesterol inhibited virus release from cholesterol-depleted cells, which suggests reestablishment of lipid raft integrity. Therefore, we examined the effect of exogenous cholesterol on the TX-100 insolubility of cell surface HA and NA. The results show that after incubation with cholesterol (0.62 mg/ml)-MβCD (10 mM) for 45 min, the TX-100 insolubility of cell

TABLE 6. Inhibition of virus release from cholesterol-depleted cells by endogenous cholesterol[a]

Initial MβCD concn (mM)	Cholesterol (mg/ml)/ MβCD(mM)	Mean (SD) relative PFU titer	Mean (SD) relative particle release
0	0/0	100[b]	100
20	0/0	327 (18)	946 (36)
20	0.62/10	10.8 (1)	48.2 (3.2)

[a] At 11 h 15 min p.i., ^{35}S-labeled virus-infected cells were treated with 20 mM MβCD for 45 min; cells were then washed and further treated with cholesterol/MβCD or mock treated for 45 min. Relative PFU titer and relative particle (HA protein band intensities) release values are presented as mean (SD) ($n = 3$).
[b] $(6.48 \pm 0.23) \times 10^7$ PFU/ml.

surface HA and NA increased and was even higher than that seen with the mock-treated cells (Table 7). Since exogenous cholesterol caused higher TX-100 insolubility of cell surface HA and NA compared to mock-treated cell results (Table 7) and reduced virus budding lower than that of mock-treated cells (Tables 5), we determined the total cholesterol content of the cells after treatment with exogenous cholesterol. The results show that after treatment with 20 mM MβCD for 45 min, the total cholesterol content was reduced to 55.9% relative to mock-treated cell levels, which is similar to the results presented in Fig. 1. After incubation of these cholesterol-depleted cells with cholesterol (0.62 mg/ml)-MβCD (10 mM) for 45 min, the total cholesterol content was increased to 293%. On the other hand, when cells were chased for 45 min without cholesterol-MβCD, the total cholesterol content (57.7%) did not change significantly compared to that of cells without chase (55.9%; Table 7). These results indicate that the higher cholesterol content of the cells after incubation with exogenous cholesterol was responsible for the higher TX-100 insolubility of cell surface HA and NA as well as the reduced release of virus particles.

Effect of HβCD and HγCD on virus budding. To examine whether the enhanced release of virus particles was mainly caused by cholesterol depletion rather than by other effects

TABLE 7. Cholesterol content and TX-100 insolubility of cell-surface HA and NA in cholesterol/MβCD-treated cells[a]

Initial MβCD concn (mM)	Cholesterol (mg/ml)/ MβCD(mM)	Mean (SD) % TX-100-insoluble protein		Mean (SD) relative cholesterol content of the cells
		HA	NA	
0	No chase[b]	ND[c]	ND	100
0	0/0	60 (3)	55 (3)	98.7 (5)
0	0.62/10	72 (4)	71 (4)	313 (19)
20	No chase[b]	34 (3)	38 (3)	55.9 (3)
20	0/0	35 (3)	40 (3)	57.7 (4)
20	0.62/10	78 (4)	75 (5)	293 (21)

[a] ^{35}S-labeled virus-infected (for TX-100 insolubility assay) or nonlabeled uninfected (for cholesterol assay) cells were mock treated (0 mM) or treated with MβCD (20 mM) at 11 h 15 min p.i. for 45 min. Cells were then further incubated for 45 min with or without cholesterol/MβCD in the medium. TX-100 insolubility of cell surface HA and NA and total cholesterol content of cells were assayed as described in Materials and Methods. Percentages are presented as mean (SD) ($n = 3$).
[b] After treatment with MβCD, cells were assayed for TX-100 insolubility and cholesterol content without further chase.
[c] ND, not done.

TABLE 8. Release of virus particles from HβCD-, HγCD-, and MβCD-treated infected cells[a]

Drug treatment and concn (mM)	Mean (SD) relative PFU titer	Mean (SD) relative particle release	Mean (SD) relative infectivity	Mean (SD) % cholesterol release
Mock	100[b]	100	1.0	0.5 (0.1)
HβCD				
10	113 (4)	120 (5)	0.94 (0.05)	17.0 (1.3)
20	190 (6)	230 (10)	0.82 (0.05)	22.5 (1.3)
30	290 (7)	417 (17)	0.69 (0.07)	27.4 (1.7)
HγCD				
10	96 (3)	98 (4)	0.98 (0.07)	1.5 (0.1)
20	97 (2)	98 (4)	0.99 (0.06)	2.9 (0.1)
30	110 (4)	112 (5)	0.98 (0.08)	3.8 (0.3)
MβCD				
10	223 (5)	742 (21)	0.3 (0.023)	30.2 (2.3)
20	137 (4)	1443 (37)	0.09 (0.002)	38.8 (2.1)
30	62 (4)	2287 (54)	0.027 (0.002)	49.8 (3.0)

[a] ^{35}S-labeled virus-infected (for virus release assay) or ^{3}H-cholesterol-labeled uninfected (for cholesterol release assay) cells were mock treated or treated with MβCD at 12 h p.i. for 45 min. Relative PFU titer, relative particle (HA protein band intensities) release, and amounts of cholesterol released after HβCD or HγCD or MβCD treatment are presented as mean (SD) ($n = 4$).
[b] $[6.87\ (0.3)] \times 10^7$ PFU/ml.

caused by the presence of cyclodextrin, we used HβCD, which releases cholesterol from cells but with lower efficiency than MβCD (2, 30), and HγCD, which does not release cholesterol from cells in significant amounts (31). The results (Table 8) show that HβCD treatment increased the release of virus particles, although less efficiently than MβCD treatment. Also, the relative infectivity of virus particles released from HβCD-treated cells was higher that that seen with MβCD-treated cells (Table 8). On the other hand, HγCD treatment did not significantly affect either the PFU titer or virus particle release compared to mock-treated cell results. As expected, HβCD (2, 30) was also less efficient than MβCD in removing cholesterol from cells and HγCD (31) did not cause any significant release of cholesterol from MDCK cells (Table 8). These results support the idea that the increased release of virus particles from MβCD-treated cells and the reduced infectivity of virus particles were caused by cholesterol depletion rather than other effects from CD.

Virus budding from MβCD-treated cells by thin-section electron microscopy. Since the budding process and release of virus particles involve the fusion of apposing cellular and viral membranes, disruption of lipid raft microdomains may affect virus morphology. Previously it was reported that MβCD treatment does not grossly affect virion morphology (46). However, as mentioned earlier, particles released from cells after exposure to a low concentration (10 mM) of MβCD treatment exhibited partially disrupted morphology (Fig. 4); such disruption was severe at higher concentrations (30 mM) of MβCD (data not shown). This can result either from defective budding or disruption of virus particles after release from the infected cells in the continued presence of MβCD in the medium or both. We therefore investigated virus budding in the presence of MβCD by thin-section EM. A representative EM micrograph (Fig. 5) shows that MβCD treatment did not affect the overall spherical morphology of the cell surface-attached virus particles. Furthermore, it should be noted that fewer virus

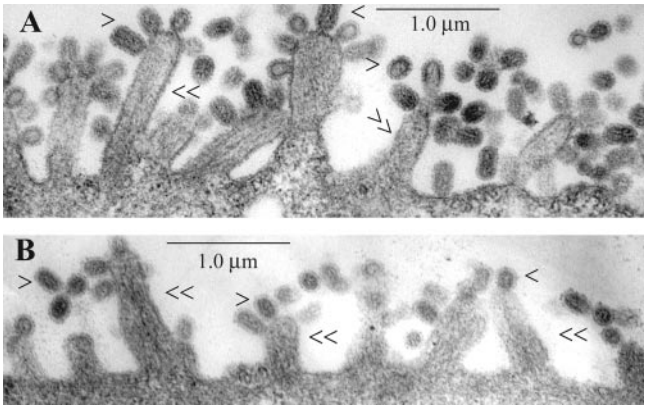

FIG. 5. Thin-section EM of budding virus particles in (A) mock-treated and (B) MβCD-treated (30 mM, 45 min) MDCK cells. Cell profiles were randomly selected and photographed at a magnification of ×19,000. single arrowheads, virus particles; double arrowheads, villi.

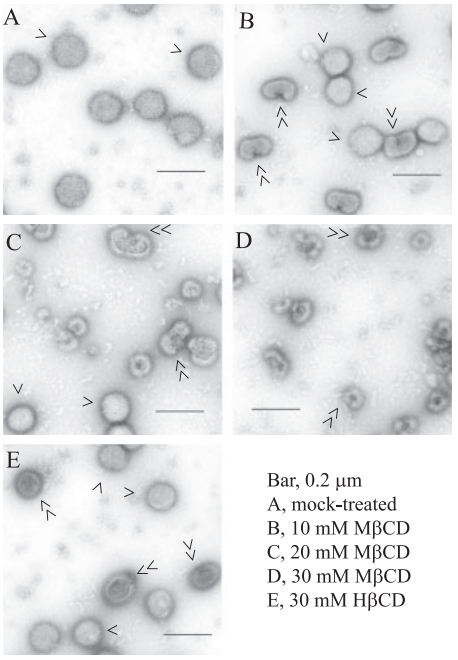

FIG. 6. Negative-stain electron microscopy of MβCD- or HβCD-treated virus particles. Virus particles were mock treated or treated with MβCD or HβCD for 30 min and were examined (photographed at ×36,000 magnification) by negative-stain EM. Single arrowheads, normal virus particles; double arrowheads, nicked or disrupted virus particles.

particles are present at the cell surface of cholesterol-depleted cells (Fig. 5), as expected, because the majority of particles would be released from MβCD-treated cells. These results indicate that disruption of virus particles likely occurred after release of virus particles in the medium containing MβCD.

Therefore, we examined the effect of MβCD or HβCD treatment on cell-free virus particles by negative-stain EM. The results (Fig. 6) show that upon treatment with 10 mM MβCD for 30 min, a significant fraction of particles exhibited a nick or hole on the envelope. These findings were similar to those reported for HIV-1 and SIV (14). With higher concentrations of MβCD, a larger fraction of particles exhibited disruption of viral envelopes (Fig. 6). However, HβCD treatment had less effect on virus particle structures. After 30 mM HβCD treatment only a small fraction of particles showed a possible nick or hole on the envelope (Fig. 6). It should also be noted that treatment with 10 mM, 20 mM, and 30 mM MβCD for 30 min reduced virus infectivity levels to about 7.1%, 1.4%, and 0.5%, respectively (Fig. 3), whereas treatment with 30 mM HβCD reduced virus infectivity to only about 31% (data not shown).

DISCUSSION

In the present study, we examined the effect of lipid raft disruption on the budding of influenza A virus in MDCK cells. The results show that lipid raft disruption by MβCD-mediated cholesterol depletion of virus-infected cells increased the release of virus particles and that disassembly of lipid rafts on the virus envelope affected integrity of viral membrane, caused leakage of viral proteins, produced nicks or holes in and disruption of the viral envelope, and adversely affected virus infectivity.

Increased release of virus particles in virus-infected cells upon disruption of lipid rafts by cholesterol depletion was a surprising observation, because lipid rafts have been implicated in virus assembly and budding (23, 24, 32, 35, 39, 47, 48). Increased release of virus particles was evident in the results of three independent assays: (i) higher PFU titers as determined by PFU assay, (ii) increased particle release as determined by protein analysis, and (iii) increased numbers of virus particles as determined by negative-stain EM. Increases in the yield of infectious virus titers were particularly evident in 10 mM MβCD throughout the treatment time (45 min). On the other hand, higher concentrations of MβCD caused an initial increase followed by a decrease in PFU titers with longer duration of treatment (Fig. 2A). However, increased particle release continued essentially in a dose-dependent manner throughout the duration (45 min) of treatment (Fig. 2B). Moreover, EM analysis confirmed the authenticity of released virus particles and showed even higher levels of particle release after MβCD treatment than that observed by protein analysis of released particles (Table 2 and 3). However, the relative infectivity of the released particles decreased at all concentrations of MβCD. Higher concentrations and longer durations of MβCD treatment caused greater decreases in the relative infectivity of released particles, suggesting the detrimental effect of MβCD on the infectivity of released virus particles (Table 3). Reductions in relative infectivity occurred partly because the particles released from cholesterol-depleted cells had reduced infectivity and partly because the infectivity of released virions decreased in the continued presence of MβCD in the medium (Table 3). The likely reason for the reduced infectivity of virus particles released from cholesterol-depleted cells in the absence of MβCD in the medium was the low cholesterol content of released virus particles. Cholesterol depletion from influenza virus envelopes has been shown to reduce infectivity (46, 47) and is discussed below. Reduced infectivity of Newcastle disease virus particles (23) and Sendai virus particles

(13) released from cholesterol-depleted cells has been reported.

In this study, we have shown that depletion of cholesterol from the viral envelope resulting from MβCD treatment caused decreases in virus infectivity. Similar effects of cholesterol depletion on influenza virus (46, 47) and HIV-I and SIV (14) were also reported earlier. However, the cause of the reduction in infectivity after cholesterol depletion remains unclear. One study showed that cholesterol depletion from the influenza viral envelope reduced levels of low pH-induced fusion at the plasma membrane (46), whereas another study found that fusion of MβCD-treated influenza viruses remained essentially unaffected (47). The present report supports the idea that the loss of integrity of viral membranes caused by cholesterol depletion and lipid raft disruption (Table 4) led to leakage of viral proteins (Table 1). Permeabilization of virion envelope and release of viral proteins after cholesterol depletion were also reported for HIV-1 and SIV (14). Furthermore, the present study showed that cholesterol depletion by MβCD caused disruption of viral structures, including nicks or holes, even at a lower concentration (10 mM) of MβCD. Therefore, release of viral proteins and disruption of particle structures are likely to be the major factors contributing to the loss of infectivity of influenza virus particles after cholesterol depletion. However, cholesterol depletion of viral membranes may also affect other steps in infection cycle, including fusion and uncoating.

It is unlikely that the enhanced release of virus particles from MβCD-treated cells reported here was caused by the effects of CD other than cholesterol depletion. First, HβCD, which is also known to release cholesterol, although less efficiently than MβCD, also enhanced virus release, and the degree of increased virus release as well as the decrease in the relative infectivity of released virions correlated to their ability to release cholesterol. Similarly, HγCD, another derivative of CD which is not known to release cholesterol significantly, did not alter either particle release or infectivity of released virions significantly. Second, increased release of virus particles correlated with lipid raft disruption as measured by the TX-100 insolubility of cell surface HA and NA. Finally, and most importantly, the presence of exogenous cholesterol was shown to reverse the effect of MβCD. Exogenous cholesterol increased the TX-100 insolubility of HA and NA and reduced the release of virus particles to a level below even that seen with mock-treated cells and partially restored the infectivity of the released virus particles. Taken together these data indicate that the increased release and decreased infectivity of virus particles from MβCD-treated cells (Table 3) were caused by cholesterol depletion and loss of lipid raft integrity.

Data presented in this study demonstrate that disruption of lipid rafts by cholesterol depletion caused an increase in the release of virus particles with reduced infectivity. This observation apparently contradicts the results reported with respect to HIV-1 (32) and Moloney murine leukemia virus (35) particle production from MβCD-treated cells. However, in those studies, conditions for MβCD treatment were different. For example, labeling of cells after cholesterol depletion (32, 35) could affect protein transport and interactions among and assembly of viral components as well as initiation of bud formation and not just bud release. On the other hand, increased particle release with reduced infectivity from MβCD-treated cells was observed for Newcastle disease virus (23). However, the lower infectivity of released virions was not directly related to their reduced cholesterol content but rather to abnormal morphogenesis of particles released from cholesterol-depleted cells (23). Similarly, based on the M protein content of released virions, increased particle release from MβCD-treated cells was observed for Sendai virus (13). Also, it is mentioned that particle release was increased after MβCD treatment of HeLa cells expressing vesicular stomatitis virus M protein (32).

Cytoskeleton disruption has been shown to affect the morphology and release of influenza virus particles (37, 45). The cortical cytoskeleton is a meshwork of actin underlying the plasma membrane. Rearrangement of the cortical actin cytoskeleton by cholesterol depletion has been demonstrated using different cell lines (10, 12). Furthermore, it was shown that cortical actin rearrangements by actin-disrupting drugs such as jasplakinolide also caused reorganization of lipid raft microdomains and increased infectious virus yield two- to threefold depending on the drug concentration (45). However, in these experiments, drug treatments were carried out throughout the infection (long treatment) and the amounts of total particle release were not quantified. Therefore, perturbation in actin cytoskeleton dynamics due to cholesterol depletion might have contributed to the enhanced release of virus particles described in the present report. Further experiments are in progress to determine the role of lipid raft disruption in the rearrangement of cortical actin network and their role in the bud pinching-off process.

Bud completion and the pinching-off process require fusion of apposing plasma membranes and viral membranes, leading to fission of virus bud and bud release. It is possible that different viruses may use different mechanisms for pinching off of virus buds, because different host proteins may be involved in this process. For example, Ono and Freed (32) observed that although wild-type HIV-1 containing PTAP late domain exhibited a decrease in particle production after MβCD treatment, PTAP minus (HIV mutant with substitutions in the PTAP sequence [32]) HIV-1 mutant- and vesicular stomatitis virus-M-mediated particle production increased after similar MβCD treatment. It also is possible that lipid rafts may have two opposite effects in the influenza A virus budding process. Initially, lipid rafts may facilitate bud formation by bringing viral components to and concentrating the components at the budding site, causing asymmetry in the membrane bilayers and favoring membrane bending and bud initiation (28). However, at the final stage of bud completion, lipid rafts may slow down and regulate bud closure. This idea is supported by the observation that exogenous cholesterol increased the TX-100 insolubility of raft-associated proteins (Table 7) and inhibited virus release (Table 5 and 6) as well. The mosaic nature of the viral membrane containing both raft-associated and non-raft-associated lipid microdomains may have different functions in the virus budding process involving bud initiation and bud closure (43). Disruption of lipid rafts at the final stage may facilitate fission and bud completion and, thereby, cause an increase in virus release.

ACKNOWLEDGMENTS

This work was supported by USPHS grants AI 16348 and AI 41681.

We thank Alicia Thompson (Center for Electron Microscopy and Microanalysis, University of Southern California, Los Angeles) for her assistance in the thin-section EM. We also thank Marianne C. Cilluffo (Microscopic Techniques and Electron Microscopy Core Facility, University of California Los Angeles) for her assistance in negative-stain EM.

REFERENCES

1. **Ali, A., R. T. Avalos, E. Ponimaskin, and D. P. Nayak.** 2000. Influenza virus assembly: effect of influenza virus glycoproteins on the membrane association of M1 protein. J. Virol. **74:**8709–8719.
2. **Atger, V. M., M. de la Llera Moya, G. W. Stoudt, W. V. Rodrigueza, M. C. Phillips, and G. H. Rothblat.** 1997. Cyclodextrins as catalysts for the removal of cholesterol from macrophage foam cells. J. Clin. Investig. **99:**773–780.
3. **Avalos, R. T., Z. Yu, and D. P. Nayak.** 1997. Association of influenza virus NP and M1 proteins with cellular cytoskeletal elements in influenza virus-infected cells. J. Virol. **71:**2947–2958.
4. **Barman, S., L. Adhikary, A. K. Chakraborti, C. Bernas, Y. Kawaoka, and D. P. Nayak.** 2004. Role of transmembrane domain and cytoplasmic tail amino acid sequences of influenza A virus neuraminidase in raft-association and virus budding. J. Virol. **78:**5258–5269.
5. **Barman, S., L. Adhikary, Y. Kawaoka, and D. P. Nayak.** 2003. Influenza A virus hemagglutinin containing basolateral localization signal does not alter the apical budding of a recombinant influenza A virus in polarized MDCK cells. Virology **305:**138–152.
6. **Brown, D. A., and E. London.** 1998. Functions of lipid rafts in biological membrane. Annu. Rev. Cell. Dev. Biol. **14:**111–136.
7. **Brown, D. A., and E. London.** 1998. Structure and origin of ordered lipid domains in biological membranes. J. Membr. Biol. **164:**103–114.
8. **Burgos, P. V., C. Klattenhoff, E. de la Fuente, A. Rigotti, and A. González.** 2004. Cholesterol depletion induces PKA-mediated basolateral-to-apical transcytosis of the scavenger receptor class B type I in MDCK cells. Proc. Natl. Acad. Sci. USA **101:**3845–3850.
9. **Carrasco, M., M. J. Amorom, and P. Digard.** 2004. Lipid raft-dependent targeting of the influenza A virus nucleoprotein to the apical plasma membrane. Traffic **5:**979–992.
10. **Chadda, R., M. T. Howes, S. J. Plowman, J. F. Hancock, R. G. Parton, and S. Mayor.** 2007. Cholesterol-sensitive Cdc42 activation regulates actin polymerization for endocytosis via the GEEC pathway. Traffic **8:**702–717.
11. **Chung, C. S., C. H. Chen, M. Y. Ho, C. Y. Huang, C. L. Liao, and W. Chang.** 2006. Vaccinia virus proteome: identification of proteins in vaccinia virus intracellular mature virion particles. J. Virol. **80:**2127–2140.
12. **Francis, S. A., J. M. Kelly, J. McCormack, R. A. Rogers, J. Lai, E. E. Schneeberger, and R. D. Lynch.** 1999. Rapid reduction of MDCK cell cholesterol by methyl-beta-cyclodextrin alters steady state transepithelial electrical resistance. Eur. J. Cell Biol. **78:**473–484.
13. **Gosselin-Grenet, A. S., G. Mottet-Osman, and L. Roux.** 2006. From assembly to virus particle budding: pertinence of the detergent resistant membranes. Virology **344:**296–303.
14. **Graham, D. R., E. Chertova, J. M. Hilburn, L. O. Arthur, and J. E. Hildreth.** 2003. Cholesterol depletion of human immunodeficiency virus type 1 and simian immunodeficiency virus with beta-cyclodextrin inactivates and permeabilizes the virions: evidence for virion-associated lipid rafts. J. Virol. **77:**8237–8248.
15. **Hanada, K., M. Nishijima, Y. Akamatsu, and R. E. Pagano.** 1995. Both sphingolipids and cholesterol participate in the detergent insolubility of alkaline phosphatase, a glycosylphosphatidylinositol-anchored protein, in mammalian membranes. J. Biol. Chem. **270:**6254–6260.
16. **Hannan, L. A., and M. Edidin.** 1996. Traffic, polarity, and detergent solubility of a glycosylphosphatidylinositol-anchored protein after LDL-deprivation of MDCK cells. J. Cell Biol. **133:**1265–1276.
17. **Harder, T., P. Scheiffele, P. Verkade, and K. Simons.** 1998. Lipid domain structure of the plasma membrane revealed by patching of membrane components. J. Cell Biol. **141:**929–942.
18. **Ilangumaran, S., and D. C. Hoessli.** 1998. Effects of cholesterol depletion by cyclodextrin on the sphingolipid microdomains of the plasma membrane. Biochem. J. **335:**433–440.
19. **Jin, H., G. P. Leser, J. Zhang, and R. A. Lamb.** 1997. Influenza virus hemagglutinin and neuraminidase cytoplasmic tails control particle shape. EMBO J. **16:**1236–1247.
20. **Keller, P., and K. Simons.** 1998. Cholesterol is required for surface transport of influenza virus hemagglutinin. J. Cell Biol. **140:**1357–1367.
21. **Kilsdonk, E. P. C., P. G. Yancey, G. W. Stoudt, F. W. Bangerter, W. J. Johnson, M. C. Phillips, and G. H. Rothblat.** 1995. Cellular cholesterol efflux mediated by cyclodextrins. J. Biol. Chem. **270:**17250–17256.
22. **Klein, U., G. Gimpl, and F. Fahrenholz.** 1995. Alteration of the myometrial plasma membrane cholesterol content with beta-cyclodextrin modulates the binding affinity of the oxytocin receptor. Biochemistry **34:**13784–13793.
23. **Laliberte, J. P., L. W. McGinnes, M. E. Peeples, and T. G. Morrison.** 2006. Integrity of membrane lipid rafts is necessary for the ordered assembly and release of infectious Newcastle disease virus particles. J. Virol. **80:**10652–10662.
24. **Leser, G. P., and R. A. Lamb.** 2005. Influenza virus assembly and budding in raft-derived microdomains: a quantitative analysis of the surface distribution of HA, NA and M2 proteins. Virology **342:**215–227.
25. **Maruyama, M., M. Kishimoto, K. Ishida, Y. Watanabe, M. Nishikawa, S. Masuda, S. R., and Y. Takakura.** 2005. Cholesterol is required for the polarized secretion of erythropoietin in Madin-Darby canine kidney cells. Arch. Biochem. Biophys. **438:**174–181.
26. **Nayak, D. P., and S. Barman.** 2002. Role of lipid rafts in virus assembly and budding. Adv. Virus Res. **77:**1977–1983.
27. **Nayak, D. P., and E.-K. W. Hui.** 2004. The role of lipid microdomains in virus biology, p. 443–491. *In* P. J. Quinn (ed.), Subcellular biochemistry, vol. 37. Kluwer Academic/Plenum Publishers, New York, NY.
28. **Nayak, D. P., E.-K. W. Hui, and S. Barman.** 2004. Assembly and budding of influenza virus. Virus Res. **106:**147–165.
29. **Neufeld, E. B., A. M. Cooney, J. Pitha, E. A. Dawidowicz, N. K. Dwyer, P. G. Pentchev, and E. J. Blanchette-Mackie.** 1996. Intracellular trafficking of cholesterol monitored with a cyclodextrin. J. Biol. Chem. **271:**21604–21613.
30. **Nguyen, D. H., Z. Liao, J. T. Buckley, and J. E. Hildreth.** 1999. The channel-forming toxin aerolysin neutralizes human immunodeficiency virus type 1. Mol. Microbiol. **33:**659–666.
31. **Ohtani, Y., T. Irie, K. Uekama, K. Fukunaga, and J. Pitha.** 1989. Differential effects of a-, b- and g-cyclodextrins on human erythrocytes. Eur. J. Biochem. **186:**17–22.
32. **Ono, A., and E. O. Freed.** 2001. Plasma membrane rafts play a critical role in HIV-1 assembly and release. Proc. Natl. Acad. Sci. USA **98:**13925–13930.
33. **Ono, A., and E. O. Freed.** 2005. Role of lipid rafts in virus replication. Adv. Virus Res. **64:**311–358.
34. **Papanikolaou, A., A. Papafotika, C. Murphy, T. Papamarcaki, O. Tsolas, M. Drab, T. V. Kurzchalia, M. Kasper, and S. Christoforidis.** 2005. Cholesterol-dependent lipid assemblies regulate the activity of the ecto-nucleotidase CD39. J. Biol. Chem. **280:**26406–26414.
35. **Pickl, W. F., F. X. Pimentel-Muinos, and B. Seed.** 2001. Lipid rafts and pseudotyping. J. Virol. **75:**7175–7183.
36. **Prydz, K., and K. Simons.** 2001. Cholesterol depletion reduces apical transport capacity in epithelial Madin-Darby canine kidney cells. Biochem. J. **357:**11–15.
37. **Roberts, P. C., and R. W. Compans.** 1998. Host cell dependence of viral morphology. Proc. Natl. Acad. Sci. USA **95:**5746–5751.
38. **Röper, K., D. Corbeil, and W. B. Huttner.** 2000. Retention of prominin in microvilli reveals distinct cholesterol-based lipid micro-domains in the apical plasma membrane. Nat. Cell Biol. **2:**582–592.
39. **Scheiffele, P., A. Rietveld, T. Wilk, and K. Simons.** 1999. Influenza viruses select ordered lipid domains during budding from the plasma membrane. J. Biol. Chem. **274:**2038–2044.
40. **Scheiffele, P., M. G. Roth, and K. Simons.** 1997. Interaction of influenza virus haemagglutinin with sphingolipid-cholesterol membrane domains via its transmembrane domain. EMBO J. **16:**5501–5508.
41. **Schmitt, A. P., and R. A. Lamb.** 2004. Escaping from the cell: assembly and budding of negative-strand RNA viruses. Curr. Top. Microbiol. Immunol. **283:**145–196.
42. **Schmitt, A. P., and R. A. Lamb.** 2005. Influenza virus assembly and budding at the viral budozone. Adv. Virus Res. **64:**383–416.
43. **Schroeder, C., H. Heider, E. Moncke-Buchner, and T. I. Lin.** 2005. The influenza virus ion channel and maturation cofactor M2 is a cholesterol-binding protein. Eur. Biophys. J. **34:**52–66.
44. **Simons, K., and D. Toomre.** 2000. Lipid rafts and signal transduction. Nat. Rev. Mol. Cell Biol. **1:**31–39.
45. **Simpson-Holley, M., D. Ellis, D. Fisher, D. Elton, J. McCauley, and P. Digard.** 2002. A functional link between the actin cytoskeleton and lipid rafts during budding of filamentous influenza virions. Virology **301:**212–225.
46. **Sun, X., and G. R. Whittaker.** 2003. Role for influenza virus envelope cholesterol in virus entry and infection. J. Virol. **77:**12543–12551.
47. **Takeda, M., G. P. Leser, C. J. Russell, and R. A. Lamb.** 2003. Influenza virus hemagglutinin concentrates in lipid raft microdomains for efficient viral fusion. Proc. Natl. Acad. Sci. USA **100:**14610–14617.
48. **Zhang, J., A. Pekosz, and R. A. Lamb.** 2000. Influenza virus assembly and lipid raft microdomains: a role for the cytoplasmic tails of the spike glycoproteins. J. Virol. **74:**4634–4644.